1st International Conference on Frontiers in Academic Research

https://www.icfarconf.com/

February 18-21, 2023, Konya, Turkey

Triple band microstrip antenna based on complementary split ring resonators for WLAN/WiMAX applications

Nail Alaoui [1*], Souad Kssena [2] Belkheiri Affaf Khouloud[3], Charef Hiba[3], Abdallah Azzouz[4], Sara Daoudi[5], Lakhdar Bouhamla[1], Umut Özkaya[6] and Enes Yiğit[7]

[1]*Laboratoire de Recherche Modélisation, Simulation et Optimisation des Systèmes Complexes Réels, University of Djelfa, Algeria.*
[2]*ETA Laboratory, Electronics Department, University of Bordj Bou Arreridj, Algeria.*
[3]*Department of Electronics and Telecommunication, University of Djelfa, Algeria.*
[4]*Advanced Electronic Systems (LSEA), Electrical Engineering Department, Faculty of Technology, MEDEA Of University, Algeria*
[5]*RCAM Laboratory Department of Electronics, Djillali Liabès University Of Sidi Bel Abbes, Algeria*
[6] *Department of Electrical and Electronics Department, Konya Technical University, Konya, Turkey*
[7] *Department of Electrical and Electronics Department, Uludağ University, Bursa, Turkey*

[*]*(alaouinail@gmail.com) Email of the corresponding author*

Abstract **–** In this paper, the design of a triple band microstrip antenna is presented for wireless communication applications. Metamaterials serve as the foundation for the triple band design, which operates at 2.4, 3.5, and 5.6 GHz. To provide the triple band response, the ground plane of a typical patch operating at 3.56 GHz is etched with two circular and one rectangular split ring resonator (SRR) unit cell. As opposed to the circular cells, which are introduced to resonate at 5.3 GHz for the higher WiMAX band, the rectangular cells are designed to resonate at 2.45 GHz for the lower WLAN band. The recommended antenna complies with WLAN and WiMAX rules and has a higher peak realized gain.

Keywords – Metamaterial, CSRR, Wimax, WLAN, Microstrip Antenna.

I. INTRODUCTION

Microstrip patch antennas are the most popular form of antenna for wireless communication systems because of its attractive qualities, such as their small weight, low profile, cheap cost, simplicity of manufacture, and compatibility with planar monolithic microwave integrated circuit (MMIC) components [1].There are several printed antenna topologies that have been created to enhance printed antenna performance. One of these topologies can be achieved, as indicated in [2], if an antenna is created for an ultra-high frequency application by modifying the geometry of the patch or by modifying the ground plane of the antenna. Through the use of various circular forms, the patch in [3] was able to achieve superior multiband antenna performance. Two different single-slotted single-band microstrip antennas were combined to form a dual-band antenna, which was another suggestion made by authors in [4].

Because of their interesting properties, metamaterials are used in a variety of applications in the realm of antenna design. [5] Many antennas based on fabricated dispersion curves (k-diagram),

split-ring resonators (SRRs), and complementary split-ring resonators (CSRRs) have been developed utilizing metamaterials. Metamaterial antennas provide a variety of techniques that may be used to improve antenna performance, such in [8], which applies the TL-MTM approach to generate a multi-band response. The metamaterial can also be utilized to increase the antenna's bandwidth and gain. In [9], the gain of the antenna is shown using metasurfaces. In [10], metamaterials may be used to change an antenna's polarization, which is a key need in several applications.

The proposed design in this study meets all requirements for the antenna to operate at WLAN and WiMAX band successfully. The complementary split ring resonator (CSRR) from MTM is the foundation of a compact, three-band microstrip antenna that is presented. The ground plane is loaded with two different geometries. In this article, a high-gain triple band microstrip antenna for WLAN and WiMAX applications is suggested.

II. ANTENNA DESIGN

The reference design is a 3.6 GHz-capable microstrip patch antenna. The patch antenna is 28 mm in width and 31 mm in length, with a copper layer thickness of 35 m.According to Figure 1, the patch radiator is printed on a Rogers RT/duroid 5880 (tm) substrate with a thickness of 1.575mm (er=0.2, tan δ =0.0009). To exactly fit the patch heater to the microstrip power supply line, which has dimensions of 4.9 mm in width and 25 mm in length, a microstrip inset power supply is given. A cut of width W0 = 5 mm is made on both sides of the feed line, and it is put into the patch with a value of Y0 = 6.5 mm. Figure 1 depicts the planned tri-band antenna arrangement.

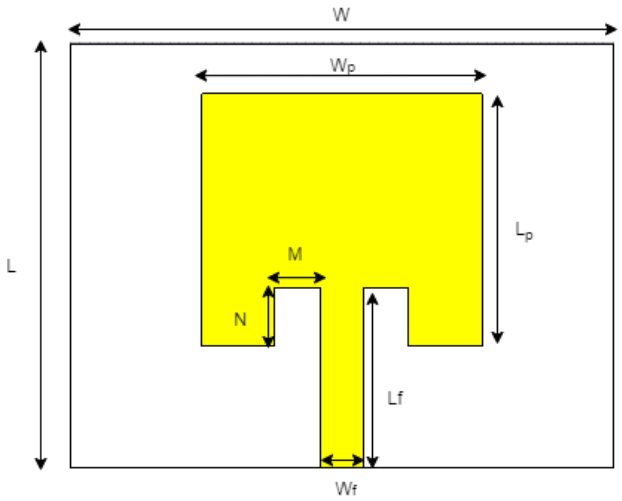

Fig1 Shows the antenna geometry of the simulation.

The ground plane is etched to create CSRRs, the complementary to basic unit cells of metamaterials, which resonate at 2.45 GHz and 5.3 GHz. In Figs. 2 and 3, the rectangular unit cell and the circular unit cell, respectively, are employed to resonate at 2.45 GHz and 5.3 GHz. By increasing the width of the unit cell as normal, the SRR's bandwidth may be expanded [37]. Because the operational bandwidth of lower WLAN (2.4 to 2.484 GHz) is less than the operating bandwidth of higher WiMAX, resonance at 5.3 GHz and 2.45 GHz is achieved using two distinct types of CSRR (5.25 to 5.85GHz). Therefore, although circular CSRR can offer a broader bandwidth than rectangular CSRR, it is not necessary to employ it to achieve 2.45 GHz resonance.

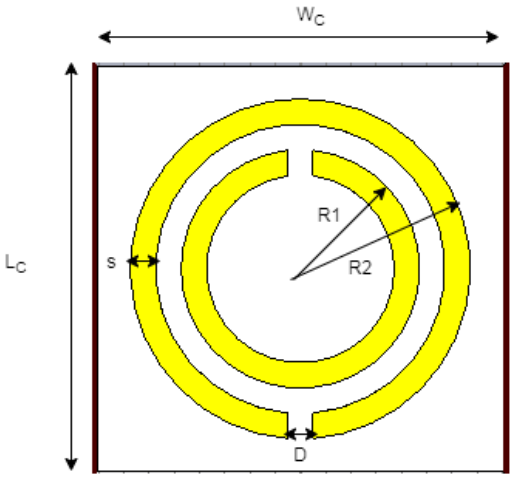

Fig.2 A circular CSRR

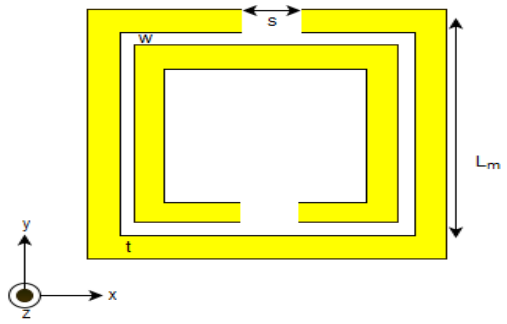

Fig.3 A rectangular CSRR

A pair of rectangular CSRRs, or circular CSRRs, are carved from the ground plane to achieve resonances at 2.45 GHz and 5.3 GHz, respectively. seen in Figure 4.

A second resonance at 2.45 GHz is produced by burying a rectangular unit cell of CSRR in the ground. The third resonance, which is 5.5 GHz, is created by etching two circular unit cells.

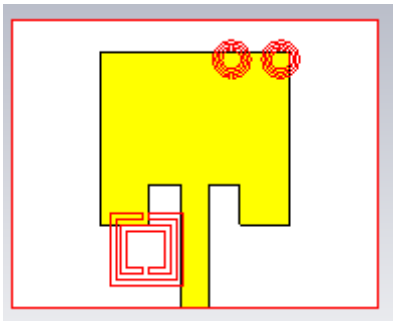

(a)

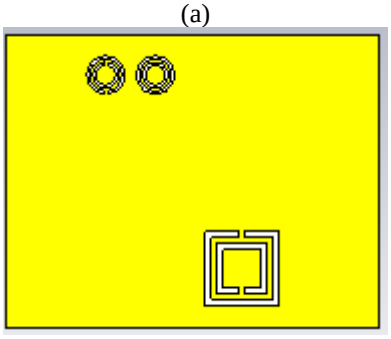

(b)

Fig.4 A rectangular patch with metamaterials

Table 1 includes a list of all the optimum antenna and unit cell dimensions.

Table 1. Dimension of first proposed antenna.

parameter	Dimensions (mm)	parameter	Dimensions (mm)
W	**60**	**L**	**47**
Wp	**31**	**Lp**	**28**
Wf	**4.9**	**Lf**	**20**
M	**5**	**N**	**6.5**
hs	**1.575**	**ht**	**0.035**

III. RESULTS AND DISCUSSIONS

Utilizing CST Microwave Studio Ver. 2014, antenna study was carried out to show simulated findings for the reflection coefficient (S11), the 2D radiation pattern, the 3D gain, and the directivity. This section provides the major simulation findings for the planned antenna.

A. *Return loss*

Figure 5 displays the simulation results for the patch antenna's return loss (S11) as a function of frequency.

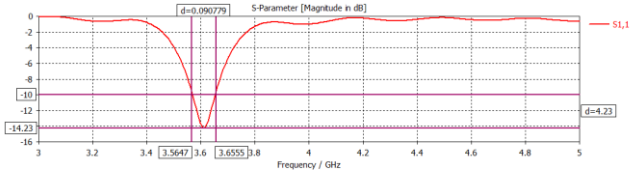

Fig5 return loss of Patch antenna

These findings demonstrate that the antenna exhibits good band adaptation in the [3.5647-3.6555GHz] range with a reflection coefficient less than -10dB. The antenna therefore has a 100 MHz bandwidth. At the frequency of 3.6 GHz, it is possible to achieve a minimum reflection coefficient of -14.23dB.

It can be shown in Figure 6 that the rectangular unit cell resonates at 2.45 GHz with a return loss of -27 dB and a shorter bandwidth, making it ideal for inferior Wlans. Figure 6 also illustrates the S-parameter characteristics of the rectangle CSRR.

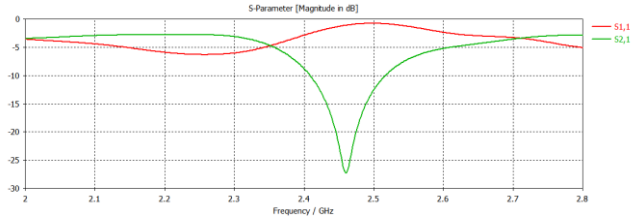

Figure 6: S-parameter of rectangular CSRR

Figure 7 displays the circular CSRR's S-parameter characteristics, and it is clear that at 5.4 GHz with a respectable bandwidth, the return loss is

less than -25 dB for future operation in the higher WiMAX band.

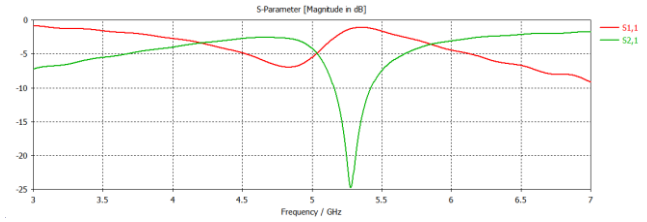

Figure 7: S-parameter of circular CSRR

The parameters of the antenna's S-parameter are shown in Figure 8. Although the overall design response suffers from frequency shift, we expected to obtain all three resonance frequencies, each of which corresponds to a different generating element. Figure 8 illustrates the coupling effect shifting the patch resonance frequency (3.6 GHz) to 3.5 GHz and the circular unit cell resonance (5.3 GHz) to 5.6 GHz.

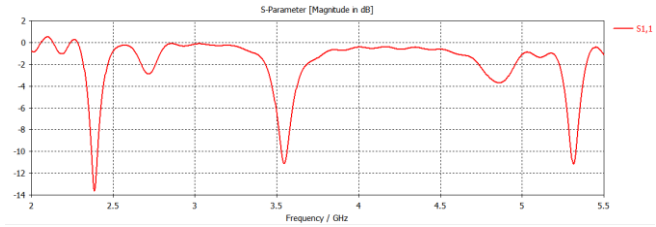

Fig.8 return loss of Proposed antenna

based on the findings, we can say that the antenna uses an excellent adaption in 3 frequencies, including wlan and wimax.

B. VSWR

The results of the simulation of the antenna standing wave ratio (VSWR) are displayed in Figure 9. The suggested antenna has a fixed wave ratio (VSWR) of 2 at operating frequencies, as shown in Fig. 9. In light of this, it can be said that the developed antenna may be effectively employed for the three frequency bands.

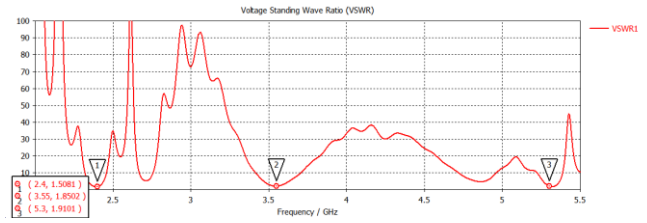

Fig. 9 proposed antenna standing wave ratio

C. *PARAMETRIC STUDY*

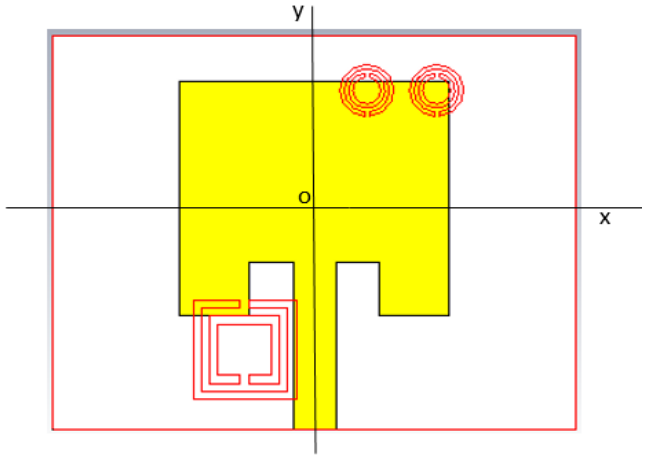

Fig.10 CRRS position survey

The parametric study in this section demonstrates the effect of the final location of the rectangular and circular unit cells on the resonant frequencies at 2.45 and 5.6 GHz (without changing the size of the cells). figure 10 illustrates.

The rectangular unit cell should be placed at this spot. X=-8 y=-16 The circular unit cell is placed in the ideal location. Both X=1 y=13 and X=10 y=13

Table 2 Optimal positions of proposed circular unit cells.

Position		**1st circular**	**2nd circular**	**gain**
state 1	**X=**	**1**	**10**	**5**
	Y=	**10**	**10**	
state 2	**X=**	**1**	**10**	**5.53**
	Y=	**11**	**11**	
state 3	**X=**	**1**	**10**	**4.90**
	Y=	**12**	**12**	
state 4	**X=**	**1**	**10**	**5.53**
	Y=	**13**	**13**	
state 5	**X=**	**1**	**10**	**5.4**
	Y=	**14**	**14**	

Table 3 Optimal positions of rectangular unit cells proposed.

Position rectangular			**gain**
state 1	**X=**	**-8**	**3**
	Y=	**-15**	
state 2	**X=**	**-8**	**3.37**
	Y=	**-16**	
state 3	**X=**	**-8**	**3.37**
	Y=	**-17**	

D. *Radiation diagram*

Given that an antenna's primary function is radiation, the radiation pattern is a crucial aspect of its functionality. An antenna radiation pattern at 2.4 GHz, 3.55 GHz, and 5.32 GHz frequencies is shown in Figures 11, 12, and 13.

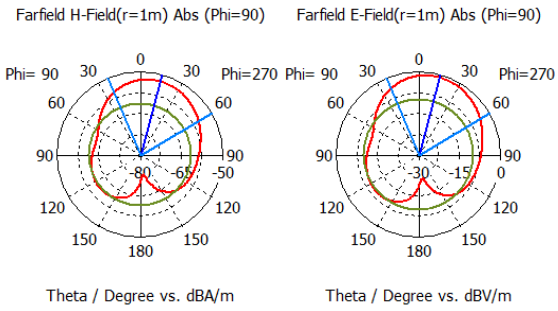

(a) (b)

Fig.11 Diagramme de rayonnement 2D en 2.4 .(a) plans E. (b) plan H

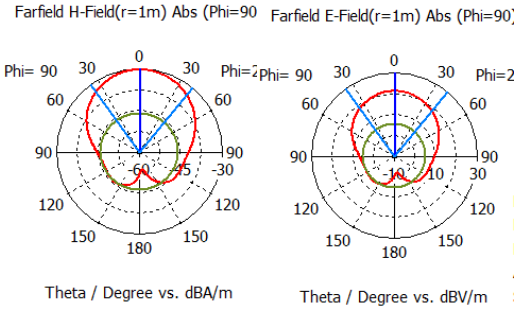

(a) (b)

Fig.12 Diagramme de rayonnement 2D en 3.5 .(a) plans E. (b) plan H

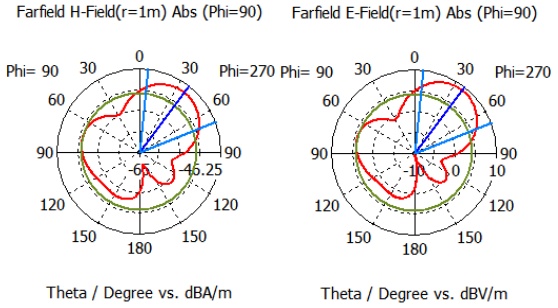

(a) (b)

Fig.13 Diagramme de rayonnement 2D en 5.5 .(a) plans E. (b) plan H

Figures 11–13 show the quasi–omnidirectional pattern that our antenna possesses in both planes (E, H). with some ripples because the etching of the three unit cells on the ground plane reduces its electrical size, which causes the reflector to be partially absent. The highest radiation is not on the flank of the two planes, as can be seen from their radiation patterns at 5.35 GHz, and this is because of the coupling effect between their two circular CSRRs.

E. *Gain*

The figure below displays the proposed antenna's 3D radiation pattern. The simulated 3D gain is displayed in Figures 14,15, and 16 to help in understanding antenna performance. As can be observed, the gain increases are 7.07 dB, 3.37 dB, and 5.53 dB for the frequencies of 3.6 GHz, 2.4 GHz, and 5.32 GHz, respectively.

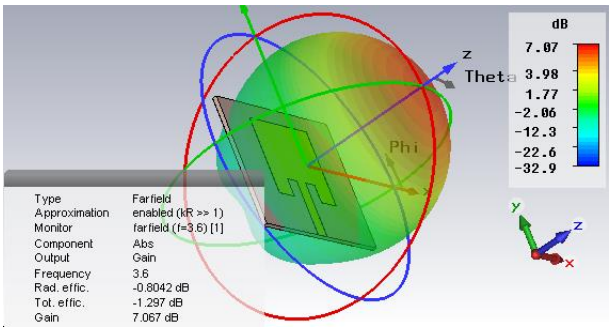

Fig.14 3D gain at 3.6 GHz

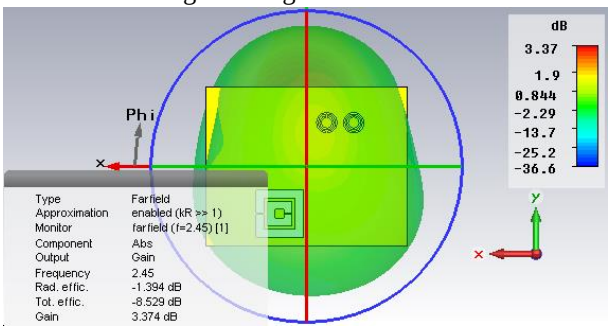

Fig.15 3D gain at 2.45 GHz

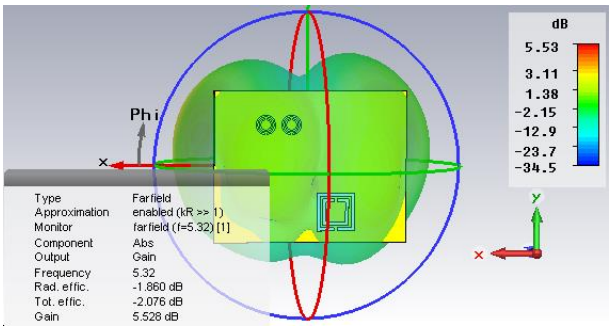

Fig.16 3D gain at 5.3 GHz

F. *Directivity*

At resonance frequencies of 3.55, 2.4, and 5.32GHz, the patch antenna utilized in WLAN/WiMAX applications provides directivity values of 7.87, 4.67 dBi, and 7.39.

Figures 17, 18, and 19 provide 3D far field radiation plots in the 2.4, 3.55, and 5.32 GHz bands, demonstrating the antenna's directed far field pattern.

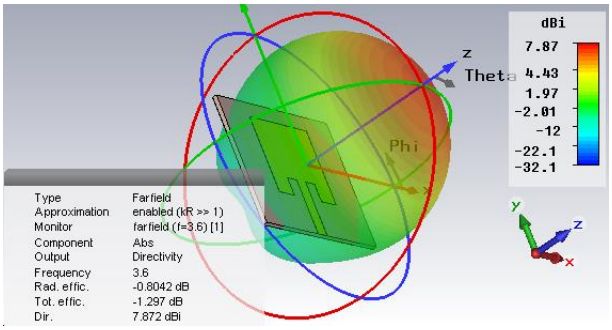

Fig.17 3D directivity at 3.5 GHz

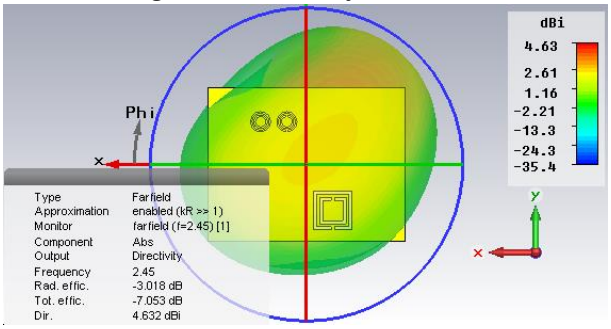

Fig18 3D directivity at 2.45 GHz

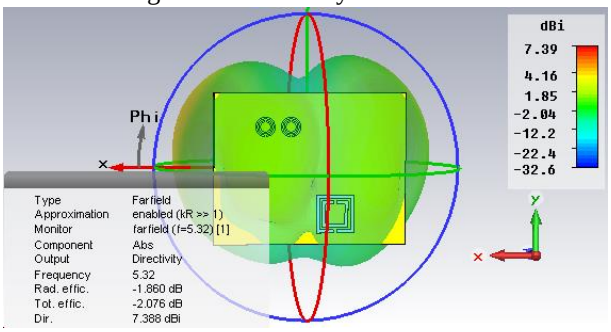

Fig.19 3D directivity at 5.32 GHz

G. *Surface current*

Figures 20, 21, and 22 depict the surface current distributions at 2.4 GHz, 3.6 GHz, and 5.32 GHz in order to more accurately describe the behavior of the proposed antenna. The intensity is maximum in the red area.

The suggested antenna's surface current density is greater at 3.6 GHz for the line, 2.4 GHz for the rectangular CRRs, and 6.8 GHz for the circular CRRS.

showing that circular CRRS are impacted by the 5.32 GHz resonance whereas rectangular CRRS are affected by the 2.4 GHz resonance.

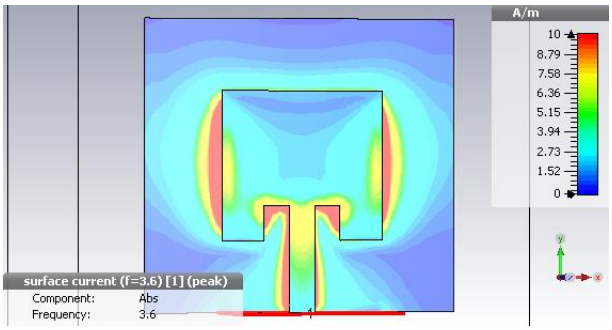

Fig.20 Proposed antenna surface current at 3.6 GHz

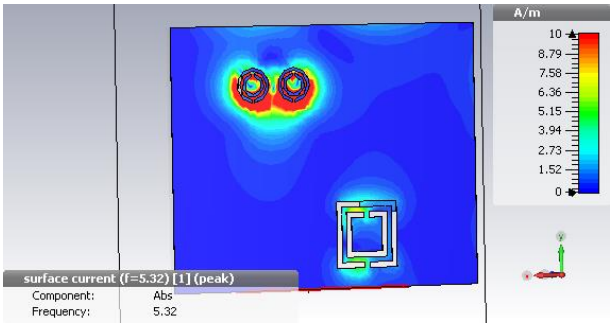

Fig.21 Proposed antenna surface current at 5.3 GHz

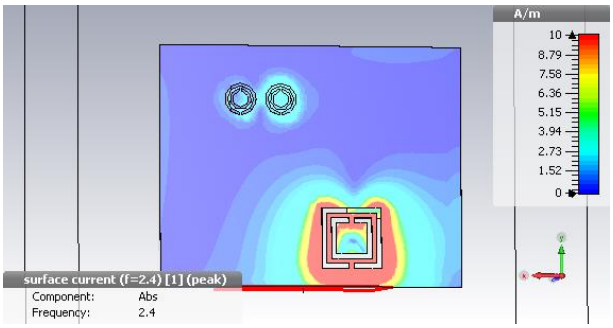

Fig. 22 Proposed antenna surface current at 2.4 GHz

The planned antenna performance is summarized in the table below:

Table 3. summary of the proposed antenna performance

F (GHz)	S11 (dB)	VSWR	Gain	Dirctivity	η
2.45	-14	1.5	3.37	4.63	72%
3.6	-11	1.85	7.07	7.87	90%
5.4	-11.3	1.91	5.53	7.39	75%

IV. COMPARISON WITH OTHER WORKS.

The proposed antenna is compared to other antennas with comparable designs and performance in table 4 below.

Regarding antenna gain and roundness, the study's suggested antenna outperformed the others.

Table 4. Comparison with other works

F(GHz)	VSWR	Gain	η	Ref

5.5		**1.14**	**86%**	
3.5	**<2**	**1.15**	**67%**	**[11]**
2.45		**1.78**	**85%**	
3.4		**0.27**	**70%**	
2.8	**<2**	**3.31**	**44%**	**[7]**
2.4		**4.45**	**78%**	
5.25		**0.90**	**96%**	
3.2	**<2**	**2.10**	**56%**	**[12]**
2.17		**2.85**	**80%**	
5.32		**5.53**	**75%**	
3.55	**<2**	**7.07**	**90%**	**Proposed**
2.4		**3.37**	**72%**	

V. CONCLUSION

Our objective was to construct a patch antenna employing supermaterials. To do this, we designed a ground-level dual CSRR circuit for the patch antenna that operates at 3.55 GHz with gains of 7.07 dBi and at 5.32 GHz with gains of 8.4 dBi (5.57dBi). Low WLAN resonance is added when the CSRR rectangular ground base is charged at (2.4 GHZ) with a gain of (3.37dBi).

REFERENCES

[1] C. A. Balanis, *Antenna theory: analysis and design*. John wiley & sons, 2015.

[2] A.-I. Petrariu and V. Popa, "Analysis and design of a long range PTFE substrate UHF RFID tag for cargo container identification," *J. Electr. Eng.*, vol. 67, no. 1, p. 42, 2016.

[3] R. Eshtiaghi, M. G. Shayesteh, and N. Zad-Shakooian, "Multicircular monopole antenna for multiband applications," *IEEE Antennas Wirel. Propag. Lett.*, vol. 10, pp. 1205–1207, 2011.

[4] U. Chakraborty, A. Kundu, S. K. Chowdhury, and A. K. Bhattacharjee, "Compact dual-band microstrip antenna for IEEE 802.11 a WLAN application," *IEEE Antennas Wirel. Propag. Lett.*, vol. 13, pp. 407–410, 2014.

[5] Y. Dong and T. Itoh, "Metamaterial-based antennas," *Proc. IEEE*, vol. 100, no. 7, pp. 2271–2285, 2012.

[6] Y. Dong, H. Toyao, and T. Itoh, "Compact circularly-polarized patch antenna loaded with metamaterial structures," *IEEE Trans. Antennas Propag.*, vol. 59, no. 11, pp. 4329–4333, 2011.

[7] Y. Dong, H. Toyao, and T. Itoh, "Design and characterization of miniaturized patch antennas loaded with complementary split-ring resonators," *IEEE Trans. Antennas Propag.*, vol. 60, no. 2 PART 2, pp. 772–785, 2012.

[8] E. Ekmekci and G. Turhan-Sayan, "Metamaterial sensor applications based on broadside-coupled SRR and V-Shaped resonator structures," *IEEE Antennas Propag. Soc. AP-S Int. Symp.*, pp. 1170–1172, 2011.

[9] Z. M. Razi, P. Rezaei, and A. Valizade, "A novel design of Fabry-Perot antenna using metamaterial superstrate for gain and bandwidth enhancement," *AEU - International Journal of Electronics and Communications*. 2015.

[10] M. Ojaroudi, M. Hassanpour, C. Ghobadi, and J. Nourinia, "A novel planar inverted-F antenna (PIFA) for WLAN/WiMAX applications," *Microw. Opt. Technol. Lett.*, 2011.

[11] N. R. Indira and A. Thenmozhi," Metamaterial Antennas Used For Wireless Applications," ARPN, Vol. 10, No. 9, May 2015.

[12] A. Gupta, S. K. Sharma and R. K. Chaudhary, "A Compact CPW-fed Metamaterial Antenna for High Efficiency and Wideband Applications," 2015 Twenty First National Conference on Communications (NCC), Mumbai, India, 2015, pp. 1-4